Multiwalled carbon nanotube - Strength to polymer composite

Jagdale Pravin[1] / Aamer. A. Khan[1] / Rovere Massimo[1] / Rosso Carlo[2] / Tagliaferro Alberto[1]

Multiwalled Carbon nanotube – Strength to polymer composite

[1] Department of Applied Science and Technology (DISAT), Politecnico di Torino, 10129, Italy, E-mail: pravin.jagdale@polito.it
[2] Department of Mechanical and Aerospace Engineering (DIMEAS), Politecnico di Torino, 10129, Italy

Abstract:
Carbon nanotubes (CNTs), a rather fascinating material, are among the pillars of nanotechnology. CNTs exhibit unique electrical, mechanical, adsorption, and thermal properties with high aspect ratio, exceptional stiffness, excellent strength, and low density, which can be exploited in the manufacturing of revolutionary smart nano composite materials. The demand for lighter and stronger polymer composite material in various applications is increasing every day. Among all the possibilities to research and exploit the exceptional properties of CNTs in polymer composites we focused on the reinforcement of epoxy resin with different types of multiwalled carbon nano tubes (MWCNTs). We studied mechanical properties such as stress, strain, ultimate tensile strength, yield point, modulus and fracture toughness, and Young's modulus by plotting and calculating by means of the off-set method. The mechanical strength of epoxy composite is increased intensely with 1 and 3 wt.% of filler.
DOI: 10.1515/psr-2015-0009

1 Introduction

Life on Earth is based on carbon. To create living matter from carbon, organisms carry out chemical reactions such as photosynthesis. This known mechanism of carbon fixation represents the largest bridge between the earth's nonliving chemistry and life. Carbon is known to be the most versatile element on earth [1]. Several allotropes of carbon are present in nature: the best known are graphite, diamond, and amorphous carbon. New nanostructured allotropes of carbon such as Bucky balls and nanotubes have been discovered in recent decades [2] and more recently other more exotic allotropes such as graphene [3, 4]. Carbon nanotubes (CNTs) are one of the fascinating carbon structures which has attracted agreat deal of attention. CNTs of a nanoscale dimension (1-D) have become well known over the past 15 years, but according to Robert Floyd Curl, Jr., (chemistry, Nobel Prize in 1996), in ancient times Indian craftsmen used nanotechnology in wootz steel as well as in paintings. Marianne Reibold et al. (University of Dresden) discovered the dispersion of CNTs in Damascus steel, famous during the middle ages, which was extraordinarily strong and flexible [5]. In 1952, the Russian scientists Radushkevich et al. published clear images of tubes made of carbon 50 nanometers in diameter [6]. The term 'nanotubes' for carbon nanotubes was first used by Wiles and Abrahamson in 1978. In 1987 Hyperion Catalysis International (USA) published a series of patents on the production and the use of 'nanofibrils' in polymers as fillers [7]. The world made an increased acquaintance with CNTs after Iijima's detailed informative rediscovery in 1991 [8]. The first observations which Sumio made were of multiwalled nanotubes [9]. Multiwalled carbon nanotubes (MWCNTs) are generally described as a type of hollow and lengthy concentric cylinder ranging from 6 to 25 or more graphite sheets on a nanoscopic level [10]. The separation between the graphene layers (interlayer spacing) is close to 0.34 nm [7, 11]. Graphene sheets are rolled at specific and discrete angles known as "chiral angles". The combination of the radius of the CNTs and the rolling angle defines the properties of the nanotube [12–15]. CNTs are available in three unique geometries (Figure 1) which are armchair (n, n), chiral (n, m) and zigzag (n, 0), the number in parenthesis indicating the number of primitive vectors needed to close the tube. Their electrical characteristics differ depending on these variations, acting either as metals or as semiconductors.

Jagdale Pravin is the corresponding author.

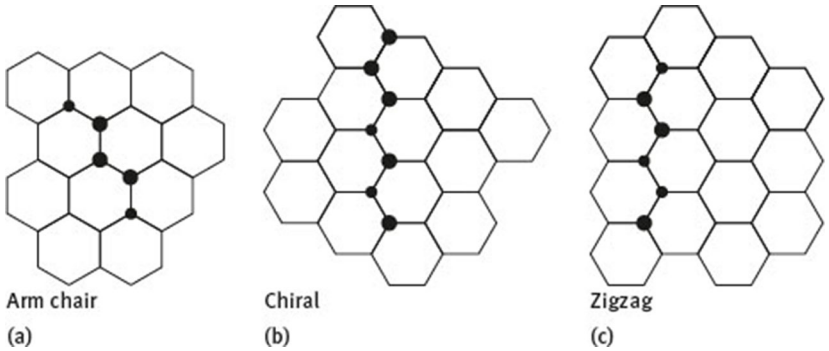

Figure 1: Different form of chirality in CNT.

Who discovered carbon nanotubes is no longer as important as who can come up with the most practical applications. CNTs can be considered to be the next generation of carbon fibers [16]. CNTs have extraordinary mechanical strength in terms of tensile strength and elastic modulus. This property also made it popular in the fields of composites. The use of CNTs as filler in composites has been given significant attention because of their remarkable thermal, mechanical, electrical, and other properties [17–19]. A variety of matrices such as ceramics, metal, and polymer for nanocomposite study has been under investigation. Polymer nanocomposites are used in all industries ranging from civil, infrastructure, automobiles, electronic equipment, aerospace, and smart textile and military equipment. Lighter and stronger materials are what is needed at present, and polymer nanocomposites are perfect for this purpose. Polymer nanocomposite materials save energy, are easy to handle and process, possess a long life, and have adequate resistance to atmospheric conditions and chemicals [16, 22, 29].

The CNT filler used for polymer nano composite have different morphology, structure, and composition [20]. Even very small volume fractions of CNT in composites dramatically alter the composite properties such as electrical, optoelectronic, thermal, and mechanical properties [21–24]. Polymer nanocomposite materials are organic polymer matrices containing dispersed inorganic/organic particulates having at least one dimension below 100 nm. The dispersion is aimed at improving the structural morphology, properties and the overall performance of the polymer (Table 1) [11, 12, 25–27]. Nanocomposites having outstanding mechanical properties and ultralight weight are already on the market [7, 20, 28–30].

Table 1 Characteristics and applications of nanofillers in polymer matrix composite materials [22].

Characteristics	Applications
Physical strength, specific toughness, light weight	Aerospace, construction, sporting goods
High dimensional stability, low coefficient of thermal expansion, low abrasion	Printed circuit boards, missile structures, aircraft brakes, aerospace antennas and support structures, large telescopes, optical benches, waveguides for stable high-frequency (gigahertz) precision measurement frames
Vibration damping, strength, toughness	Audio equipment, including microphones and speakers; robotic arms
Electrical conductivity	Airframes and aircraft skin materials, novel tooling, casings and bases for electronic equipment, electromagnetic interference (EMI) and radio frequency (RF) shielding, brushes
Low biological reactivity, permeability by x-rays	Medical prostheses, surgery and x-ray equipment, implants, tendon/ligament repair
Fatigue resistance, self-lubrication	General engineering applications with moving parts, such as automobiles
Low chemical reactivity, high corrosion resistance	Chemical exposure; radiation fields; valves, seals, and pump components
Electromagnetic properties	Electronic devices; motor and generator parts; radiological equipment

As we are considering nanocomposites based on epoxy resin, let us spend a few words on it here. The first commercial exploration of the properties of epoxy resins was by I.G. Farben Industries in Germany during the 1930s, and from that time on epoxy resins have been put to industrial uses more than any other resins. Epoxy resins adhere well to a wide variety of reinforcing agents. Their very low shrinkage [31–33] make them popular

in composite industry. Epoxy resins in a cured state are very resistant to chemical influences and offer excellent electrical insulation.

The rising global demand for industrial applications like aerospace and wind energy industries is propelling research in epoxy resin composites. Epoxy resin-based composites provide flexibility and reduction of the overall weight of the material, enhancing the creep and fatigue resistance. The main applications of epoxy resin are found in formulations for mortars, screeds, and polymer concretes for adhesion primers and coatings in civil as well as mechanical engineering for corrosion protection [13], etc. Epoxy composites are used in specialized sophisticated structures and are the preferred choice where functionality is most importanct [34]. Epoxy resins do have some disadvantages, e.g. they are sensitive to moisture, and the heat distortion point, the dimensions, and the physical properties decrease with moisture take-up. High temperature affects their toughness: they have a high coefficient of thermal expansion when compared to other thermosets, are sensitive to UV, etc. There is still much need for researching and exploiting the exceptional properties of MWCNTs in epoxy polymer composites to tackle such limitations.

The focus in this chapter is on the reinforcement of epoxy resin with several types of MWCNTs to study their mechanical properties such as stress, strain, ultimate tensile strength, yield point, modulus, and fracture toughness.

2 Material and methods

2.1 Epoxy resin in general

Epoxy resins are thermosetting polymers that contain an epoxide ring of the basic functional group. The basic raw materials required for the production of epoxy resins include bisphenol A (BPA), epichlorohydrin, phenols, aromatic amines, and aliphatic alcohols. Epoxides are three-membered rings with two carbon atoms and one oxygen atom (Figure 2).

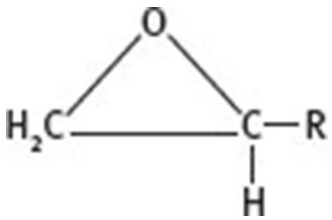

Figure 2: Epoxide ring.

Epoxides can be classified as difunctional to polyfunctional epoxides. A curing agent/cross linker hardens the epoxides without releasing any byproduct compounds and with a minimal shrinkage to form a rigid material bearing high resistance to solvents and stable dimensions at elevated temperatures. Diglycidyl ether of bisphenol A with its repeating units is the most widely used difunctional epoxy, as shown in the Figure 3.

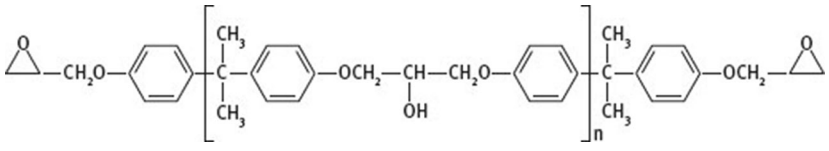

Figure 3: Di-functional epoxy resin.

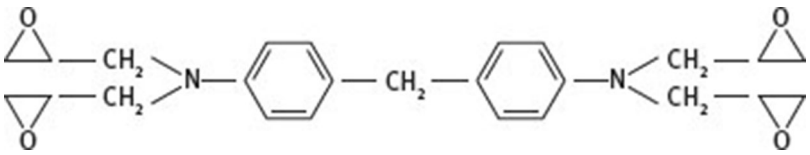

Figure 4: Tetraglycidyl Methylene Dianiline (TGMDA).

Polyfunctional epoxy with aromatic and heterocyclic glycidyl amine groups are used for high-temperature aerospace applications. These compounds contain tetraglycidyl methylene dianiline, (TGMDA) groups which guarantee performance in such conditions [31, 32].

2.2 Epoxy resin in sample preparation

Commercially modified Epilox resin (T 19-36/700, LEUNA-Harze GmbH, Germany) was used for this study. It is a colorless, low viscosity (650–750 mPa/s at 25 °C) epoxy resin with a reduced crystallization tendency and a density of 1.14 g · cm^{-3}. Its chemical composition is Bisphenol-A epichloro hydrine (50–100 wt.%) and oxirane, mono-{(C12-14-alkyloxy) methyl derivatives (10–25 wt.%). To complete the polymerization reaction, a cross linker was used.

Epilox cross linker (H10-31, LEUNA-Harze GmbH, Germany) is a liquid, colorless, low viscosity (400–600 mPa s) modified cycloaliphatic polyamine epoxide adduct with a density of 1 g · cm^{-3} and containing 3-aminomethyl-3,5,5-trimethylcyclohexyl (25–50 wt.%), benzyl alcohol (25–50 wt.%), and nonyl phenol (<5 wt.%). 3-amino-methyl-3,5,5-tri-methylcyclohexyl was in a clear liquid with a density (0.24 g/ml at 200°C).

2.3 Multi walled carbon nanotubes (MWCNTs)

MWCNTs can be synthesized by various processes. The three most widely used methods are visible light vaporization, arc discharge, and catalytic chemical vapor deposition (often abbreviated to chemical vapor deposition (CVD)).

The visible-light method can be further classified into three separate methods of synthesis namely: (i) laser ablation, in which a pulsed laser is used to carry out the synthesis of carbon nano tubes, (ii) a continuous laser is used for synthesis in laser vaporization method, while in (iii) the solar vaporization method a continuous multiwavelength light from a solar furnace source is used to carry out the process. Other methods used to synthesize CNTs are flame synthesis, liquid hydrocarbon synthesis, and catalytic plastic pyrolysis. These methods are not used for bulk production, so they are of less significance compared to the widely-used CVD method.

CVD is a thermal reaction in which a gaseous hydrocarbon is cracked into carbon and other constituents in the presence of a catalyst. The catalyst is usually a transition metal such as cobalt, iron, or nickel. The MWCNT growth reaction is aided by a catalyst. In-house MWCNT growth was performed by using iron as a catalyst along with camphor (Sigma Aldrich 99 % purity) and waste polyethylene granules as a carbon source. The system was set to adopt the floating catalyst method. In the floating catalyst method, the metal particles are transferred by an inert gas carrier (argon/helium) to a nonreactive silicon dioxide surface. The temperature of the reactor is adjusted in a way that allows the cracking of the carbon source but not the pyrolysis of the carbon-containing species. For a given combination of the catalyst and gas mixture that is effective in producing carbon nanotubes, MWCNTs formation is favored for the formation of SWCNTs at a lower temperature range of 700~800 °C and at a high temperature range of 850~950 °C. The main advantage of this system is that it can easily be scaled to commercial scale CNT production [7, 11, 12, 15]. This method was adopted to synthesize MWCNTs (FCCF340 and P3) in house (carbon group, Politecnico di Torino). Commercial functionalized and graphitized MWCNTs were purchased from Cheaptubes, USA, and normal MWCNTs (MW7) were provided by Nanothinx, Greece. The detailed specifications of MWCNTs are listed in Table 2.

Table 2 MWCNTs characterisation.

Code	Type	Diameter nm	Length μm	Purity weight %
MW7	MWCNTs	25~45	<10	98.5
MWF3	-COOH functionalized	<8	10~30	95
MWG2	Thin craphitized	8~15	10~50	99
FCCF340	In-house made from camphor	50	179	85

2.4 MWCNT Nanofiller epoxy composite preparation

Dispersion of the nano scale filler in the polymer matrix plays a key role in determining composites properties. Nano scale fillers exhibit a surface area of several orders of magnitude larger than the surface area possessed by microscale particles. The surface area of CNTs behaves as an interface to transfer the stress from polymer matrix to the individual nanotube and dissipate the effect of the load applied. But in nanoscale particles secondary forces are prevalent, and for this reason CNTs have a strong tendency to form agglomerates. Exploitation of the remarkable properties of CNTs in polymers is therefore dependant on their homogeneous dispersion in

the polymer matrix, good breaking up of the carbon nanotube agglomerates, and adequate wetting of CNTs with polymer. Parameters that affect the quality of dispersion are length, purity, surface modification such as functionalization, graphitisation such as the degree of entanglement, polymer viscosity [15, 20, 23, 29]. This is why we choose different kinds of MWCNTs to study the mechanical behavior in epoxy polymer. Good dispersion of MWCNTs in polymer matrix can be achieved by either mechanical or chemical means. In the first case MWCNTs can be dispersed into low-viscosity liquids (either polymer or cross linker) by using mechanical shear mixing before polymerisation starts.

2.5 Preparation of epilox CNT nanocomposites

Epoxy resin (LEUNA-Harze GmbH, T 19-36/700) (63 wt.%), cross linker (LEUNA-Harze GmbH, H 10–31) (37 wt.%) and filler CNTs (1 and 3 wt.%) (as shown in Table 3) were thoroughly mixed with mechanical stirring (20,000 RPM for 2 min). High-speed mechanical mixing initiates the exothermic polymerisation between the resin and cross linker, resulting in evolving entrapped gas bubbles in the composites. Sonication (ultrasonic frequency 37 kHz for 15 min) followed by degassing in the vacuum (50 mbar for 30 min) steps have been subsequently undertaken in order to get rid of these entrapped gas bubbles before the composite completes its polymerisation reaction. Before the onset of polymerization, the composite mixtures were moulded into dog-bone shapes (ASTM D 638 standard) as shown in Figure 5. Handling strength of these composite occurred in 24 h (with temperature >25 °C), and complete curing was achieved after 5–7 days at 25 °C. To cure the moulds faster, however, they were kept in the oven at 70 °C for 4 h. As mentioned earlier the composites were prepared with 1 and 3 wt.% of MWCNT filler concentrations. Before beginning analysis, the thickness, width, and length of the composite samples were measured. These dimensions were approximately (±0.1 mm) the same for each sample. Defective samples (with uneven surfaces and surface-entrapped air bubbles) were not considered for further analysis.

Table 3 Epoxy and epoxy composite component quantity required (in grams).

Epoxy composite	*Epoxy resin (g)*	*Cross linker*	*Filler*
Blank	63	37	–
1% Filler	62.37	36.63	1.0
3% Filler	61.11	35.89	3.0

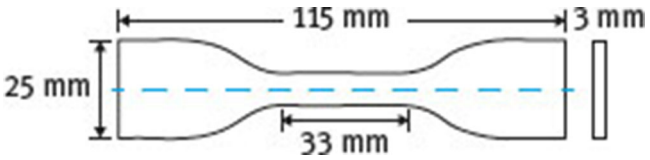

Figure 5: Schematic diagram of dog-bone shaped composite samples for mechanical analysis.

3 Mechanical analysis

For mechanical testing we used a Q-test 10 tensile tester by MTS, a very flexible machine. It can be used to investigate the mechanical properties of materials ranging from plastics to composite materials to metals. It is equipped with multiple jaws to hold the material specimens. The machine can be provided with several load cells, ranging from 50 N to 10 kN. In the reported tests the machine was equipped with a 10 kN load cell. The machine is also equipped with an extensometer and automatic control systems. The distance between the jaws can be adjusted manually. The machine operates on the working principle of a constant rate of traverse ranging from 0.025 mm/min to 1 m/min. One jaw is fixed at the bottom while the top jaw pulls the specimen upwards it and measures the reaction force by means of the load cell. The specimen is stretched at a uniform deformation velocity until it breaks. The load and elongation graphs are displayed on the computer screen attached to the machine, and these data are exported to an ASCII file for subsequent analysis. The whole arrangement is shown in Figure 6.

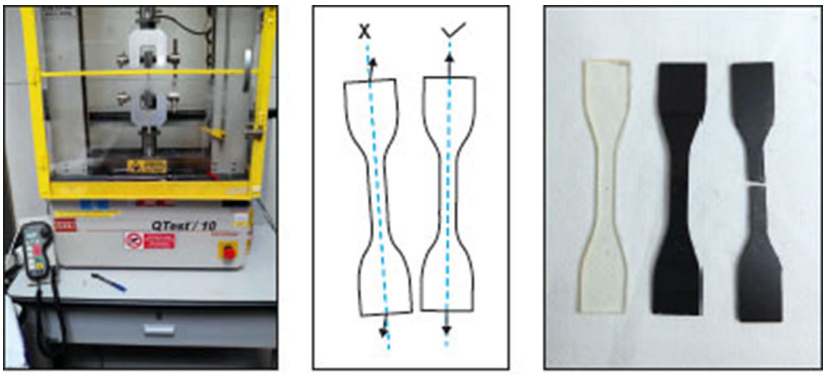

Figure 6: (a) Q-test 10 analysis instrument; (b) proper sample fixing; (c) actual sample for analysis.

The traverse speed is set before testing the specimen. The value was set at 0.5 mm/min traverse speed. The software requires the dimensions of the test specimen to be according the ASTM D-638 standard. The dimensions provided for analysis were the length, measuring length, thickness, and width of the specimen. Mechanical data (tensile load F vs. displacement d) obtained from instrumental software was further elaborated to determine elongation, stress, strain, Young's modulus, and fracture toughness values.

As a first step the load and displacement values were converted to stress (MPa) and strain (adimensional), respectively. The average stress σ is defined as "the ratio of the tensile load applied to the area of the original cross section"[35]:

$$\sigma = \frac{F}{S_{initial}}. \tag{1}$$

Strain is a dimensionless quantity that describes the ratio of change in length (d) to the original length of composite [35]

$$\varepsilon = \frac{d}{L_{initial}}. \tag{2}$$

Stress vs. strain plots are the most common way of reporting data. A typical data plot (see Figure 7) can be divided in three regions:

(1) *elastic region*: the linear (or quasi-linear) reversible part at low strain; removing the stress will bring back the specimen to the initial geometry;

(2) *plastic region*: departure from linearity occurs and irreversible elongation enters into play; a permanent elongation remains even if the stress is removed;

(3) *fracture region*: the final part of the plot leading to specimen failure through fracture.

In order to classify the materials and to better describe their behavior, several quantities are commonly defined and reported. The relevant quantities (see Figure 7) are as follows:

(1) *Young's modulus (E)*: its value corresponds to the slope of the fitting line of the elastic region and gives information on the elasticity and rigidity of the material

(2) *Yield point*: around this point a transition from elastic to plastic behavior occurs. The yield point is conventionally defined as the point of intersection between the material curve and a line parallel to the elastic one having an offset strain of 0.2 %. The coordinates of the yield point give the information about *yield stress* (σ_Y) and *yield strain* (ε_Y). Higher values σ_Y and ε_Y mean a higher load-bearing capability in the elastic region. These two quantities directly affect the capability of the material to absorbing energy in the elastic region

(3) *Modulus of resilience* (u_o). Resilience describes the ability of the material to absorb energy while being deformed elastically, and return the supplied energy on unloading. It corresponds to the maximum value of the elastic energy density that the material can withstand before the onset of plastic deformation. The parameter u_o can be calculated evaluating the area under the stress-strain curve from the origin to the yield point, approximately equal to

$$u_o = \frac{1}{2}\sigma_y \varepsilon_y = \frac{1}{2}\frac{\sigma_y^2}{E} \tag{3}$$

(4) *Ultimate strength point*: this is the point with the maximum stress value on the stress-strain curve. A further increase of strain leads to relevant shrinking of the specimen section ultimately leading to fracture

(5) *Ultimate tensile strength* (UTS, also known as "tensile strength"): this is the stress value that corresponds to the ultimate strength point. Its value in a composite is affected by preparation method, defects in the material, and temperature of the material and the environment

(6) *Fracture point*: this is the last point recorded for the stress-strain curve before specimen failure. Strain at fracture point (also: strain at break) defines the ability of a material to elongate under tensile loads. It also expresses the capability of a material to resist changes of shape without crack formation.

(7) *Fracture toughness* (K, also known as "toughness"): this is the amount of energy density the material can absorb before fracture occurs. Hence it describes the ability of a material to absorb energy and deform plastically without fracturing. Its value is the area under the stress-strain curve from the origin to the fracture point displacement ε_f

$$K = \int_0^{\varepsilon_f} \sigma \, d\varepsilon. \tag{4}$$

A dedicated software has been developed in-house that automatically identifies all the relevant points and calculates the relevant quantities of the stress-strain curve.

The two extreme behaviors of materials are ductile (Figure 7) and brittle (Figure 8). In the first case, after the ultimate strength point there is a wide plastic region. In the second case, the failure occurs just after the end of the elastic region (i.e. the fracture point is very close to the yield point and corresponds also to the ultimate strength point). Plastic region is almost absent.

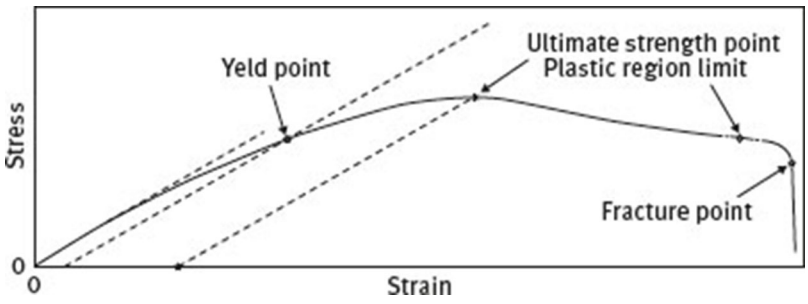

Figure 7: Ductile behavior.

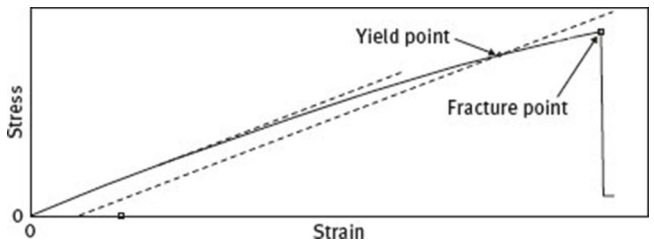

Figure 8: Brittle behavior.

4 FESEM details with sample preparation

A ZEISS SUPRA™ 40 field emission scanning electron microscope (FESEM) was used to deliver high quality and high resolution images of nanoscale materials to meet the demands and challenges involved in the study

of application of nanoscale materials. The mechanically fractured composite part was chosen for analysis. Generally the specimens to be analysed are prepared by cryofracturing them in liquid nitrogen. In this study, we prefer to cut the samples close to a mechanically broken part. Care was taken to keep the mechanically modified surface untouched and undamaged in sample preparation. The samples were mounted on aluminum studs in order to be able to observe them from a top view. A chromium coating of 5–7 nm thickness was deposited by electron sputtering to avoid the charging effect.

FESEM analysis of epoxy polymer shows the slipping of the polymeric chain during the application of the tensile force which causes the composite to break. The epoxy fractured surface (Figure 9) is more uniform and defect free, which is ideally a benchmark condition for mechanical property of polymeric sample.

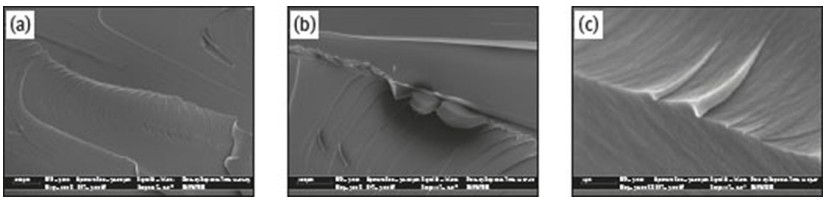

Figure 9: FESEM analysis of the epoxy resin specimens.

5 Results and discussion

All the produced specimens were tested, and the data were collected and analyzed. In the following the different behaviors of the specimens are highlighted, the presence of MWCNTs, is shown in the FESEM images of the fracture region for each specimen type, and conclusions are drawn.

The first analyzed group of specimens is the MW7. In Figure 10 the tensile behavior of this group is compared with the blank epoxy. In Figure 11 the FESEM analysis is represented for showing the presence of MWCNTs. This approach is used also for the other group of specimens.

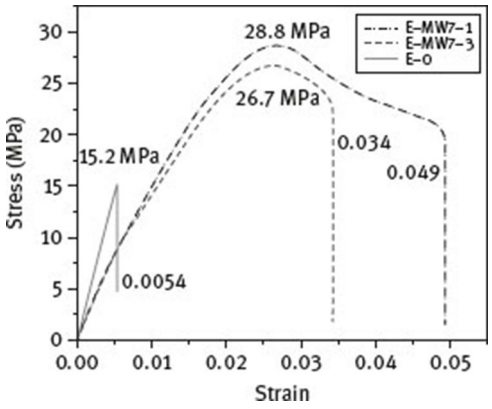

Figure 10: Tensile behavior of MW7.

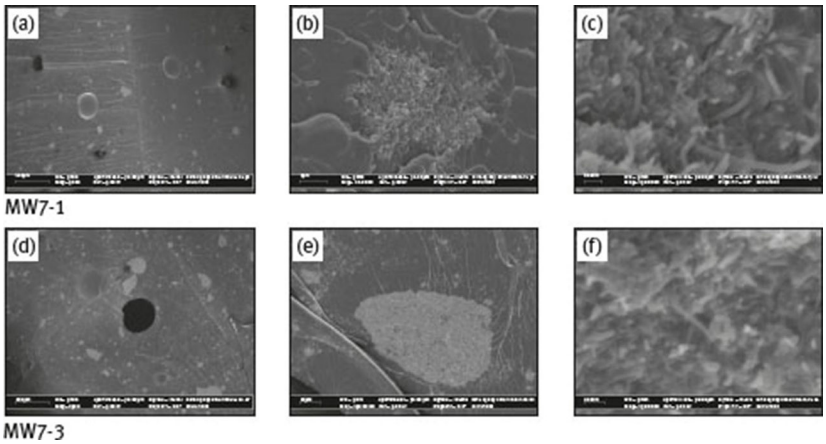

Figure 11: FESEM of MW7 specimens: CNTs are clearly visible in the rightmost column.

Composites prepared with MW7 show the presence of microbubbles. They create a weak point for fracture, leading to a premature failure of the composite during the course of the application of stress. The microbubble size is larger in 3 % MW7 sample, with a consequent reduction of the plastic region. Moreover, MW7 CNTs have a tendency to form big chunks due to Van der Waal's forces (MW7 and also MWG2-1).

The agglomerations have a great impact on localizing the mechanical forces to create a fracture point during the course of elongation by a tensile force. Chunks also reduce the ability to stop the slippage of the polymer chains one over another. We speculate that the two phenomena can be related, with big chunks leading to bubble formation during the preparation procedure (the reasons for this still need to be investigated). On the basis of Figure 10, it is possible to conclude that the MW7 group presents an increment of the UTS and a reduction of the Young's modulus with respect to the blank epoxy. In addition, a change of the behavior from brittle to ductile can be underlined.

The same analysis is made for the MWF3 specimen group (Figure 12 and Figure 13). The two percentages of CNTs lead to remarkably different behavior. The MWF3-3 specimen presents a brittle behavior, while the MWF3-1 has a more plastic one. The analysis of FESEM images suggest that the reason for that behavior may be related to the presence of chunks. On the other hand the values of the yield stress and Young's modulus of the two specimens are similar, suggesting that the main effect on the elastic region is saturating at low CNT contents.

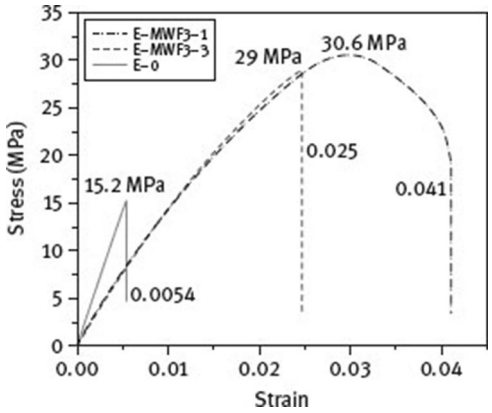

Figure 12: Tensile behavior of MWF3.

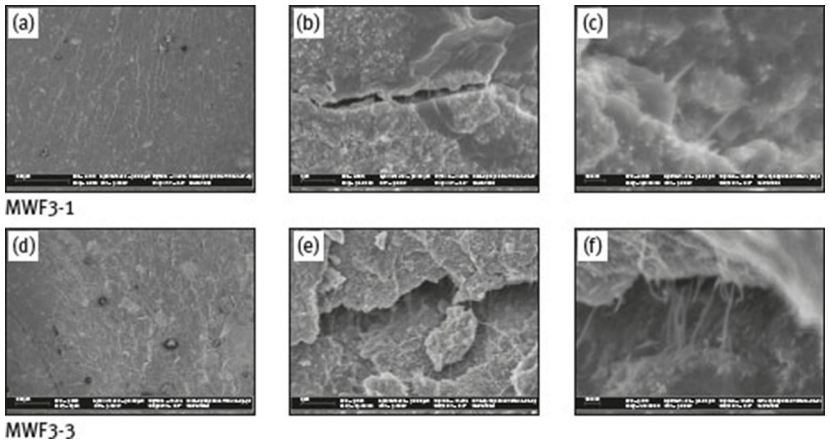

Figure 13: FESEM of MWF3 specimens: CNTs are clearly visible in the rightmost column.

By considering the curves of the thirdgroup (MWG2 specimens, Figure 15 and Figure 16), we observe that the introduction of MWCNTs in the epoxy matrix changes the behavior of the material from brittle to ductile, increases the UTS, and decreases the Young's modulus, as depicted for the previous groups. In this case the higher values of UTS and toughness are reached at a lower filler percentage, but the material with higher percentage of filler presents a higher Young's modulus and a lower UTS and toughness with respect to the other filler percentage.

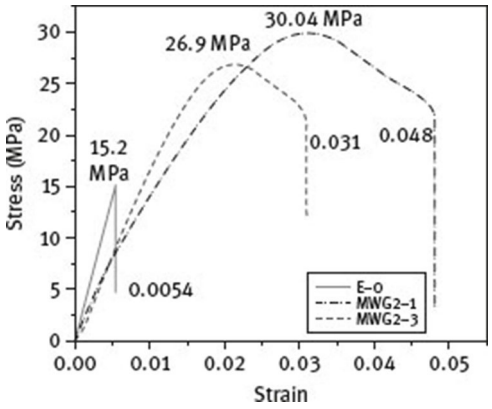

Figure 14: Tensile behavior of MWG2.

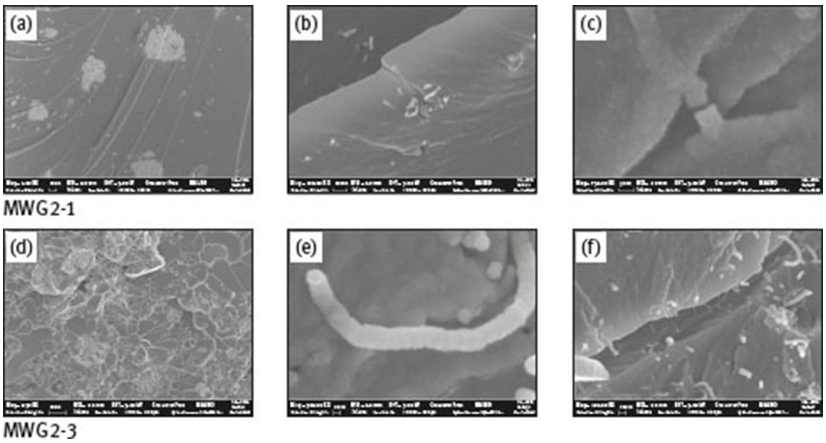

Figure 15: FESEM of MWG2 specimens: CNTs are clearly visible in the rightmost column.

The FCCF340 group presents a perfect ductile behavior and no great difference in terms of toughness. A little increase of UTS and Young's modulus is presented by the specimen with more filler (3 %) (see Figure 16 and Figure 17).

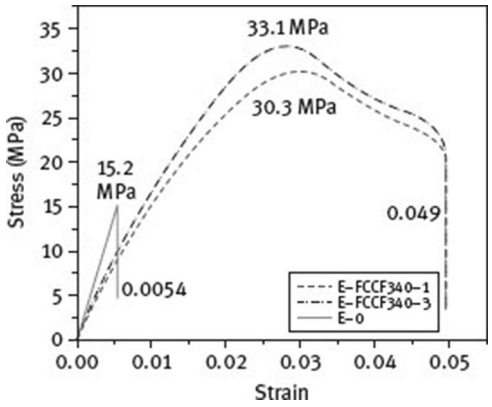

Figure 16: Tensile behavior of FCCF340.

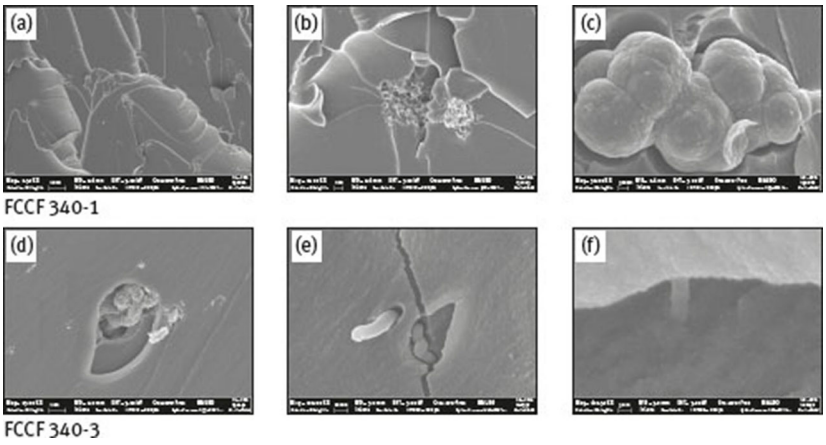

Figure 17: FESEM of FCCF340 specimens: CNTs are clearly visible in the rightmost column.

Good and evenly distributed filler (made and functionalized in-house) MWCNTs add to the strength of the polymers and enhance the load-carrying capacity. In this case it seems that there is a good interaction between the filler and the polymer matrix. There is significant interfacial bonding between the filler and the matrix. The stress is transferred from the matrix to the filler particles, and the particles help transfer this stress to single fibres, thus adding to the strength of the composite. A functionalized MWCNTs (MWF3) family has better tensile properties due to the better interaction between the filler and the matrix, thus preventing these layers from slipping over each other during the application of the tensile force. Whereas in-house made MWCNTs (FCCF340) have a high aspect ratio, with some round shape carbon growth which allows for better interaction with epoxy resin result in getting better or comparable mechanical property than other MWCNT families tried in this study.

By comparing all the extracted data, some additional considerations can be taken.

6 Ultimate tensile stress (UTS)

The comparative study of UTS (Figure 18) shows that MWCNTs of all kinds enhance the UTS from 15.2 MPa (epoxy polymer) to 26–33 MPa. The maximum UTS was observed for in-house made MWCNTs (FCCF340) with 3 wt.%. So in terms of UTS it is possible to conclude that the MWCNTs, independent of their type and percentage, can nearly double the UTS of the matrix material.

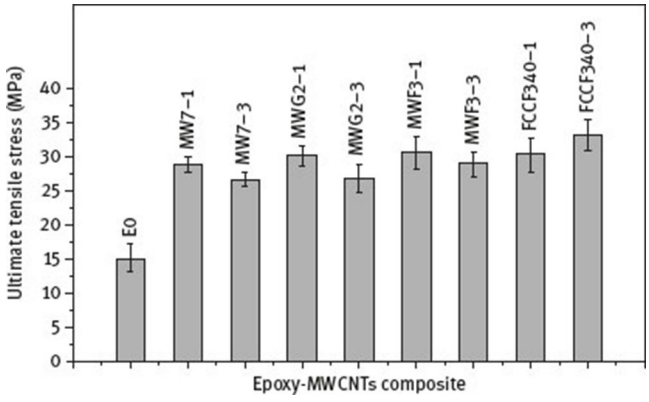

Figure 18: Ultimate tensile strength comparisons.

6.1 Strain at break

Almost 10 time better elongation under stress is observed (Figure 19) in comparison with epoxy polymer and composite with in-house made CNTs FCCF-340 (1 and 3 wt.%), Normal MW7 (1 wt.%) and graphitized MWG2 (1 wt.%) nanofillers. This means that the filler increases the plastic region of the matrix material, increasing the capability of the material to withstand a crack without failing.

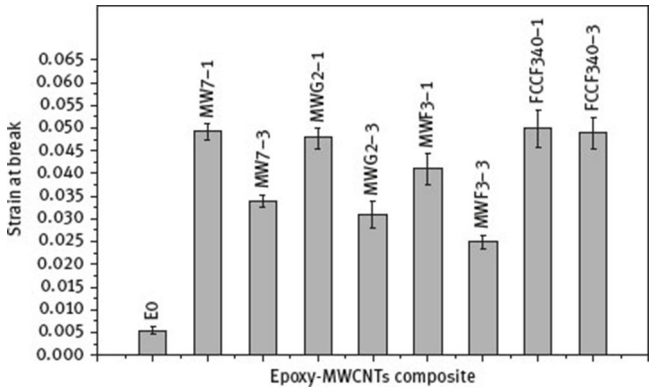

Figure 19: Strain at break comparison.

6.2 Yield point

The ductile material, as the composite material that experiences a plastic zone in the stress-strain chart, is usually preferred for the design of mechanical and structural component, because a "reservoir" of strength is guaranteed by the plastic region. In fact, the ultimate tensile strength (UTS) is usually higher than the yield limit, so fixing the yield limit as the failure threshold, before having the complete failure of the structure there is an additional increment of force. The design criteria are based on the yield limit, so this value indicates the capability of the material to last. As an example, consider a shaft for transmitting a torque. If the shaft is made in pure epoxy without filler, the nominal transmitted torque can be considered as reference and set to 1 Nm. If thesame shaft is made of epoxy filled with MWCNT, the transmitted torque increases to at least 2.4 Nm (MW7-3). This means that the same shaft with the same weight can transmit more than double the reference torque.

By analyzing Figure 20, it is possible to highlight that the presence of the filler almost always more than doubles the yield stress. A small variation with respect to the filler percentage can be seen. In fact, for MW7, MWG2, and MWF3 a 1 % filler amount leads to higher values of yield stress with respect to the 3% case. The trend is inverted for FCCF340, as it occurs for traditional fillers in plastic material.

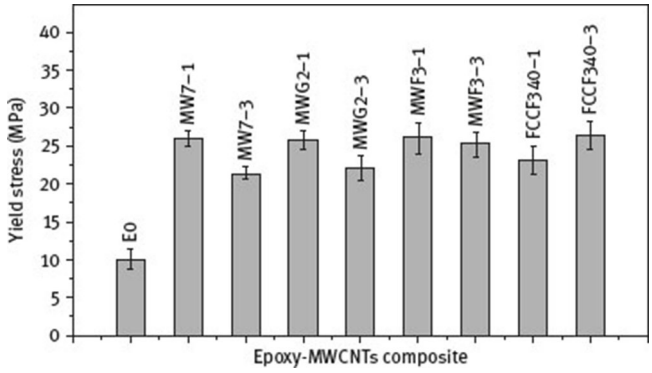

Figure 20: Yield stress comparison.

6.3 Resilience

The highest value of resilience was shown by the MWF3 group with 1wt.% CNT addition (Figure 21). Multiwall graphitized MWCNTs (MWG2-1) in 1 wt.% showed the second best results, as depicted in the graph. The resilience could be considered as an indicator of the elastic capability of the material. Let us consider the same shaft as above. The higher the resilience of the material, the higher is the elastic energy accumulated during the loading process, so that a higher resilience material allows us to design a shaft that, with the same external load, deforms less, or, with the same size of the shaft, can accumulate more energy. This means that the presence of MWCNTs inside the epoxy resin increases the possibility of accumulating elastic energy in the material.

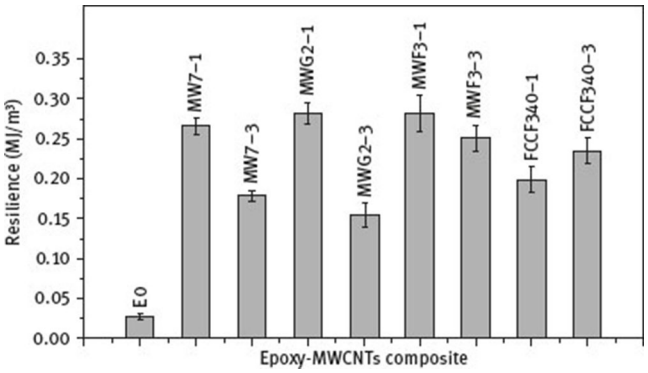

Figure 21: Resilience comparison.

6.4 Toughness

Higher toughness indicates that a higher energy per unit volume can be absorbed in the plastic region before breaking. The best results were shown by the in-house generated MWCNTs (FCCF340-3) in 3% by weight of the composite. Multiwall graphitized CNTs showed the second-best results. An impact test is required for obtaining fully reliable information about the fracture behavior, but the higher the toughness, the higher is the capability of the material to guarantee safety of the design, because a great plastic energy amount is present. On the basis of Figure 22 and Figure 10, Figure 12, Figure 14, and Figure 16 we can clearly see evidence of the brittle or ductile behavior of the different materials. Referring to Figure 10, Figure 12, Figure 14, and Figure 16, the base epoxy and MWF3-3 do not show a relevant plastic region, so they can be considered as brittle (in fact they have lower values of toughness). On the basis of the chart in Figure 22 a threshold for transition between brittle and ductile behavior could be set at 0.5 MJ/m^3. If the material has toughness lower than this value, it can be considered as brittle; otherwise it presents an important plastic behavior.

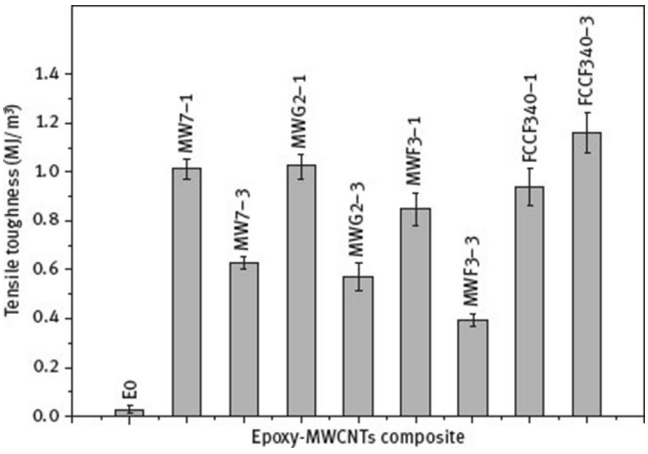

Figure 22: Tensile toughness comparisons.

6.5 Young's modulus

The highest value of Young's modulus (1850 MPa) was obtained (Figure 23) by the composite prepared by graphitized MWCNTs (MWG2-3) with 3 wt.% of filler, but it is still approximately 1000 MPa less than the epoxy resin. The second-best results were shown by in-house generated MWCNTs (FCCF340-3) with 3% by weight of filler. The value for Young's modulus was 1700 MPa.

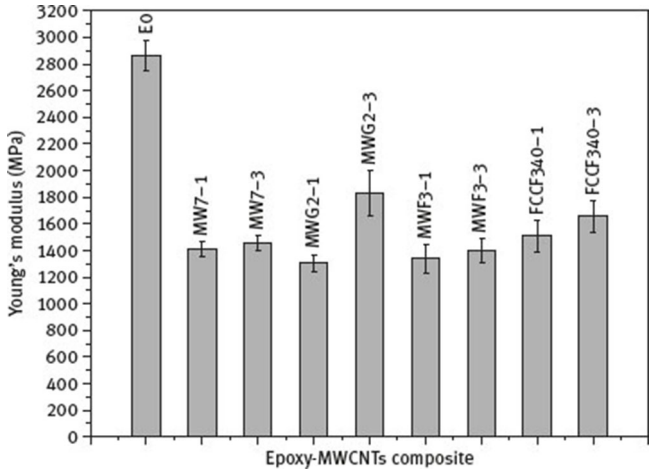

Figure 23: Young's modulus comparison.

Overall mechanical results show that in most of the analysis in-house made MWCNTs (FCCF340) show better or comparable results as compared to commercial MWCNT nanofillers. It is possible to underline that the presence of the filler decreases in the same manner as the Young's modulus, more or less halving it.

7 Conclusions

As highlighted in the previous discussion, the presence of MWCNTs inside epoxy resin changes its behavior from brittle to ductile and increases the UTS and the yield stress, but it decreases the Young's modulus. The mechanism that justifies this variation is probably relatedto the MWCNTs capability to block the crack propagation and support the sliding of the polymeric chain. So the stress for breaking the material is increased, the plastic deformation is favored, but at the same time the polymeric chain tends to slide instead of react, so the Young's modulus lowers.

MWCNTs with different surface modification with higher aspect ratios (length to diameter ratio) showed improvement in the tensile properties. Better MWCNT dispersion (less agglomeration) and less or no defect may better achieve improved mechanical strength. In-house made MWCNTs with cheaper sources have better or comparable mechanical properties, like commercial MWCNTs in composites. The nanostructural dimensions have a great impact on dispersion in the matrix, which will continue to impact on the mechanical property of the composite.

This work suggests that the presence of small quantities of MWCNT could drastically change the behavior of the epoxy resin and open the way for a series of new possible applications of this material.

8 Future trends

- The rheological behavior of carbon nanotubes reinforced polymer composites has not been studied thoroughly until now. Investigation in this area will aid in the further improvement of the properties of the polymer composite.
- CNTs can be used to substitute carbon fibers and carbon black in many applications.
- There is much room for work in the areas of CNT-polymer composites prepared by coagulation, solution processing, and in-situ polymerization.
- Comparison should be done with other mechanical dispersion techniques such as calendaring and sonication in order to find the best possible way to have a good even dispersion of the carbon nanotubes in the polymer matrix.
- Cheaper and higher production of CNTs is needed to further increase the market share in the composites sector.

Acknowledgement

We thank Dr. Salvatore Guastella (Polytechnic of Turin, Italy) for valuable discussion, Nanothinx for providing their CNTs, and LEUNA-Harze GmbH, Germany for epoxy resin. We also thank the Higher Education Commission (HEC) of Pakistan for their financial support for Mr. Aamer during the course of his research work.

This article is also available in: Charitidis, Nanomaterials in Joining. De Gruyter (2015), isbn 978-3-11-033960.

References

[1] Paradise M, Goswami T. 2007. Carbon nanotubes – Production and industrial applications, *Mater. Des.* **28**(5), 1477–1489.
[2] Kroto HW, Heath JR, O'Brien SC, Curl RF, Smalley RE. 1985. C60: Buckminsterfullerene, *Nature* **318**(6042), 162–163.
[3] Harris PJF. 2004. Fullerene-related structure of commercial glassy carbons, *Philos. Mag.* **84**(29), 3159–3167.
[4] Iijima S. 1980. Direct observation of the tetrahedral bonding in graphitized carbon black by high resolution electron microscopy, *J. Cryst. Growth* **50**(3), 675–683.
[5] Reibold M, Paufler P, Levin AA, Kochmann W, Pätzke N, Meyer DC. 2006. Materials: carbon nanotubes in an ancient Damascus sabre, *Nature* **444**(7117), 286.
[6] Radushkevich LV, Luk'yanovich VM. 1952. The structure of carbon forming in thermal decomposition of carbon monoxide on an iron catalyst, *Sov. J. Chem. Phys.* **26**, 88–95.
[7] Mcnally T, Pötschke P. 2011. *Polymer-Carbon Nanotube Composites*, Series in. Cambridge, UK, Woodhead Publishing Limited.
[8] Iijima S. 1991. Helical microtubules of graphitic carbon, *Nature* **354** 56–58.
[9] Burstein E. 2003. A major milestone in nanoscale material science: the 2002 Benjamin Franklin Medal in Physics presented to Sumio Iijima, *J. Franklin Inst.* **340**(3–4), 221–242.
[10] Yamabe T. 1995. Recent development of carbon nanotube, *Synth. Met.* **70**(1–3), 1511–1518.
[11] Grady BP. 2011. *Carbon Nanotube-Polymer Composites: Manufacture, Properties, and Applications*, Unabridged, New Jersey, Johne Wiley & Sons Inc.
[12] Dai H. 2002. Carbon Nanotubes: Synthesis, Integration, and Properties, *Acc. Chem. Res.* **35**(12), 1035–1044.
[13] Kalamkarov AL, Georgiades AV, Rokkam SK, Veedu VP, Ghasemi-Nejhad MN. 2006. Analytical and numerical techniques to predict carbon nanotubes properties, *Int. J. Solids Struct.* **43**(22–23), 6832–6854.
[14] Cao G, Chen X. 2007. The effects of chirality and boundary conditions on the mechanical properties of single-walled carbon nanotubes, *Int. J. Solids Struct.* **44**(17), 5447–5465.
[15] Shaffer MSP, Sander JKW. 2006. Carbon nanotube/nanofibre polymer composites, in S.G. Advani (ed.), *Processing and Properties of nano composites*, World Scientific Publishing Co. pvt. Ltd., 1–59.
[16] Song K, Zhang Y, Meng J, Green E, Tajaddod N, Li H, Minus M. 2013. Structural Polymer-Based Carbon Nanotube Composite Fibers: Understanding the Processing–Structure–Performance Relationship, *Materials (Basel).* **6**(6), 2543–2577.
[17] Bokobza L. 2007. Multiwall carbon nanotube elastomeric composites: A review, *Polymer (Guildf).* **48**(17), 4907–4920.
[18] Fiedler B, Gojny FH, Wichmann MHG, Nolte MCM, Schulte K. 2006. Fundamental aspects of nano-reinforced composites, *Compos. Sci. Technol.* **66**(16), 3115–3125.
[19] Her S-C, Lai C-Y. 2013. Dynamic Behavior of Nanocomposites Reinforced with Multi-Walled Carbon Nanotubes (MWCNTs), *Materials (Basel).* **6**(6), 2274–2284.
[20] Du F, Fischer JE, Winey KI. 2003. Coagulation method for preparing single-walled carbon nanotube/poly(methyl methacrylate) composites and their modulus, electrical conductivity, and thermal stability, *J. Polym. Sci. Part B Polym. Phys.* **41**(24), 3333–3338.
[21] Ash BJ, Siegel RW, Schadler LS. 2004. Glass-transition temperature behavior of alumina/PMMA nanocomposites, *J. Polym. Sci. Part B Polym. Phys.* **42**(23), 4371–4383.
[22] Ash LSSBJ, Eitan A. 2004. Polymer nanocomposites with particle and carbon nanotube fillers, in KPA Schwarz, CI. Contescu (eds.), *Dekker Encyclopedia of Nanoscience and Nanotechnol-ogy*, 1st ed., New York, Marcel Dekker, 2917–2930.
[23] Coleman JN, Khan U, Blau WJ, Gun'ko YK. 2006. Small but strong: A review of the mechanical properties of carbon nanotube–polymer composites, *Carbon N. Y.* **44**(9), 1624–1652.
[24] Ramana VG, Balaji P, Kumar N, Jain P. 2010. Mechanical properties of multi-walled carbon nanotube reinforced polymer composites, *Indian J. Eng. Mater. Sci.* **17**(210), 331–337.
[25] Park C, Wilkinson J, Banda S, Ounaies Z, Wise KE, Sauti G, Lillehei PT, Harrison JS. 2006. Aligned single-wall carbon nanotube polymer composites using an electric field, *J. Polym. Sci. Part B Polym. Phys.* **44**(12), 1751–1762.
[26] Hashim A (Ed.). 2011. *Advances in Nanocomposite Technology*. InTech.
[27] Reddy B (Ed.). 2011. *Advances in Nanocomposites – Synthesis, Characterization and Industrial Applications*, InTech.
[28] Wenjie Wang NSM. 2007. Characterization of NanotubeReinforced Polymer Composites, in DS Yellampalli (ed.), *Carbon Nanotubes – Polymer Nanocomposites*, 1st ed., Croatia: InTech, 155–172.
[29] Bal S. Samal SS. 2007. Carbon nanotube reinforced polymer composites – A state of the art, *Bull. Mater. Sci.* **30**(4) 379–386.
[30] Zanello LP, Zhao B, Hu H, Haddon RC. 2006. Bone cell proliferation on carbon nanotubes, *Nano Lett.*, **6**(3), 562–567.
[31] Xanthos M (Ed.). 2010. *Functional Fillers for Plastics*, 2nd ed. John Wiley & Sons Inc, 531.
[32] Akovali G (Ed.). 2001. *Handbook of composite fabrication*, Illustrate. iSmithers Rapra Publishing, 196.
[33] Andrews R, Weisenberger M. 2004. Carbon nanotube polymer composites, *Curr. Opin. Solid State Mater. Sci.* **8**(1), 31–37.
[34] May C (Ed.). 1987. *Epoxy Resins: Chemistry and Technology*, 2nd ed. CRC Press, 1288.
[35] Davis JR. 2004. *Tensile Testing*, 2nd ed. ASM International, 279.